Synthetic and Systems Biotechnology 9 (2024) 842–852

Contents lists available at ScienceDirect

Synthetic and Systems Biotechnology

journal homepage: www.keaipublishing.com/en/journals/synthetic-and-systems-biotechnology

Original Research Article

Comparative omics directed gene discovery and rewiring for normal temperature-adaptive red pigment synthesis by polar psychrotrophic fungus *Geomyces* sp. WNF-15A

Haoyu Long [a,1], Jiawei Zhou [a,1], Yanna Ren [a,**], Jian Lu [a], Nengfei Wang [b,***], Haifeng Liu [c], Xiangshan Zhou [d], Menghao Cai [a,e,*]

[a] State Key Laboratory of Bioreactor Engineering, East China University of Science and Technology, Shanghai, 200237, China
[b] School of Chemistry & Chemical Engineering, Linyi University, Linyi, 276005, China
[c] China Resources Angde Biotech Pharma Co., Ltd., 78 E-jiao Street, Liaocheng, China
[d] China Resources Biopharmaceutical Co., Ltd., 1301-84 Sightseeing Road, Shenzhen, China
[e] Shanghai Collaborative Innovation Center for Biomanufacturing, Shanghai, 200237, China

ARTICLE INFO

Keywords:
Polar fungi
Red pigment
Cold-adaptive
Comparative omics
Food additives

ABSTRACT

The Antarctic fungus *Geomyces* sp. WNF-15A can produce high-quality red pigments (AGRP) with good prospects for the use in food and cosmetic area. However, efficient AGRP synthesis relies on low-temperature and thus limits its industrial development. Here genome sequencing and comparative analysis were performed on the wild-type versus to four mutants derived from natural mutagenesis and transposon insertion mutation. Eleven mutated genes were identified from 2309 SNPs and 256 Indels. A CRISPR-Cas9 gene-editing system was established for functional analysis of these genes. Deficiency of *scaffold1.t692* and *scaffold2.t704* with unknown functions highly improved AGRP synthesis at all tested temperatures. Of note, the two mutants produced comparable levels of AGRP at 20 °C to the wild-type at 14 °C. They also broke the normal-temperature limitation and effectively synthesized AGRP at 25 °C. Comparative metabolomic analysis revealed that deficiency of *scaffold1.t692* improved AGRP synthesis by regulation of global metabolic pathways especially downregulation of the competitive pathways. Knockout of key genes responsible for the differential metabolites confirmed the metabolomic results. This study shows new clues for cold-adaptive regulatory mechanism of polar fungi. It also provides references for exploitation and utilization of psychrotrophic fungal resources.

1. Introduction

Polar regions, including the Antarctic, the Arctic and their surrounding areas, represent one of the most inhospitable regions in the earth. Due to the special geographical locations, these regions carry fragile ecosystems against harsh environments, *e.g.*, extremely low temperatures, acid-base stress, repeated freeze-thaw cycles, high winds, high salinity, and high radiation [1,2]. Therefore, organisms living in the polar regions must have the ability to deal with these adverse conditions [3].

Recent studies have shown that microorganisms surviving in the polar regions are not only diverse in species but also abundant in numbers. For instance, filamentous fungi and yeasts distributed widely in Antarctica [4]. Polar fungi can synthesize a variety of new secondary metabolites with good biological activities such as antiviral, antifungal, antiprotozoal, antitumor, *etc.* [5–12]. To adapt with the extreme environments, they have evolved to special metabolic features with functions of cold-active enzymes, antifreeze proteins, antioxidants, pigments, *etc.* [13–18]. These kinds of products hold good potential to be used in pharmaceutical, food and cosmetic areas [19]. Nevertheless,

Abbreviations: AGRP, Antarctic *Geomyces* red pigment; Δ1–692, knockout of *scaffold1.t692* (this naming rule is also applicable to other genes).

Peer review under responsibility of KeAi Communications Co., Ltd.

* Corresponding author. State Key Laboratory of Bioreactor Engineering, East China University of Science and Technology, Shanghai, 200237, China.
** Corresponding author.
*** Corresponding author.
E-mail addresses: yannaren@ecust.edu.cn (Y. Ren), wangnengfei@lyu.edu.cn (N. Wang), cmh022199@ecust.edu.cn (M. Cai).
[1] co-first author.

https://doi.org/10.1016/j.synbio.2024.07.002
Received 13 May 2024; Received in revised form 11 July 2024; Accepted 12 July 2024
Available online 16 July 2024

marketed products derived from polar microorganisms are currently quite limited. Their specific phenotypes such as psychrotrophilism and slow growth usually bring great difficulties for artificial culture especially in industrial-scale fermentation.

The polar fungus *Geomyces* sp. WNF-15A is a typical psychrotrophic mould isolated from the Antarctic soil. It can synthesize a kind of Antarctic *Geomyces* red pigment (AGRP) consisted of polysaccharides, geomycamine and its derivatives [20–22]. The AGRP is easily soluble in water and its extinction coefficient is even higher than that of the *Monascus* red pigment (for low-end use) and cochineal red pigment (for high-end use) on the market [23]. In addition, it shows better stability in reducing agents, food additives, acid and alkali environments, as compared to cochineal red pigment, and has good tolerance to ultraviolet rays, oxidants, and metal ions [23]. The toxin citrinin commonly produced by *Monascus* spp. was not detected from *Geomyces* sp. WNF-15A [22,24]. The median lethal dose (LD50) of the AGRP was over than 15,000 mg kg^{-1}, which also meets level 1 of the acute toxicity dose classification of food toxicology (non-toxic) in China [24]. Therefore, it holds great potential to be developed as an alternative red pigment product in food and cosmetic applications. Nevertheless, the psychrotrophic traits of *Geomyces* sp. WNF-15A brings great difficulties for the production of the AGRP in large-scale culture. Generally, the wild-type strain tends to synthesize the AGRP below 14 °C, but the production decreased by 60 %–70 % when temperature rose to 20 °C and almost completely blocked at 25 °C [21,22,25]. The low-temperature maintenance under cold condition brought about high-cost and control difficulties.

To break the cold-dependent AGRP production, we used atmospheric and room temperature plasmas mutagenesis to improve AGRP production adapted for normal temperature. A mutant strain *Geomyces* sp. WNF-15A-M210 (M210, similar designating mode hereinafter) with an efficient AGRP production at 20 °C was obtained from thousands of colonies finally [21]. We further involved transposon insertion mutation in the wild-type strain to unlock AGRP synthesis under normal temperature. Finally, single and dual systems of transposable insertion were established with fungal transposons of *Helitron*, *Fot1*, *Impala*, *Minos* and *Restless*, respectively. From dozens of mutants, the MP14 and MPS1 produced high-level AGRP at 20 °C, and meanwhile, the mutants of MP2, MP10, MPS3, MPS4, MPD1 and MPS1 synthesized AGRP at 25 °C slightly [22,25]. These achievements indicated that the underlying repression mechanism of AGRP synthesis responsive to normal temperature was broken. Tracking of the mutated sites in the genome may help discovery of the target genes that regulating AGRP synthesis responsive to temperature variation.

Nowadays, omics technologies have been widely used for revealing the hidden targets and exploring the interactions between multiple substances in biological systems. With multi-omics in hand, scientists can explore the differentially expressed genes between comparative samples in various fields [26–30]. It will further direct the rational rewiring of the host and obtain specific phenotypes, which is also known as inverse metabolic engineering in molecular breeding area [31,32]. In this study, we aim to identify the mutated sites in the genome by comparative genomic analysis of the wild-type and normal temperature-adaptive mutant strains. Functions of the mutated genes were then verified by gene knockout and replenishment, and the functional genes were modified to release the AGRP synthesis under normal temperature. The high-production strain was subjected to metabolomic analysis to illustrate how the functional gene affect cell metabolism. This study offers reference for the exploration of other polar microbial and product resources.

2. Materials and methods

2.1. Strains, media, and culture conditions

The wild-type *Geomyces* sp. WNF-15A and its mutant strains (M210, MPS1, MPS3 and MPS4) were stored in 20 % (w/v) glycerol at −80 °C [22,25]. Engineered strains in this work were summarized in Table S1. *Escherichia coli* Top 10 was preserved in our laboratory. The Luria-Bertani medium [10 g L^{-1} NaCl, 10 g L^{-1} tryptone, 5 g L^{-1} yeast extract and 20 g L^{-1} agar (for solid medium)] was used for *E. coli* culture. The YPD medium (10 g L^{-1} yeast extract, 20 g L^{-1} tryptone, 20 g L^{-1} glucose) was used to culture fungal strains for the extraction of their genomes. The seed culture medium for the fungal strains consisted of 10 g L^{-1} glucose, 20 g L^{-1} maltose, 20 g L^{-1} mannitol, 10 g L^{-1} sodium glutamate, 6 g L^{-1} yeast extract, 0.3 g L^{-1} $MgSO_4{\cdot}7H_2O$, and 0.5 g L^{-1} KH_2PO_4. For agar plate culture, medium was prepared by adding 30 g L^{-1} agar into the seed medium. For submerged culture, medium S that developed previously (28 g L^{-1} soluble starch, 1.5 g L^{-1} tryptone) was used and 20 glass beads (diameter of 4 mm) were added to disperse the fungal mycelia [21]. Besides, 0.016 g L^{-1} NaH_2PO_4 and 0.927 g L^{-1} Na_2HPO_4 was supplemented when fermented in bioreactor.

For culture of the *Geomyces* strains, 100 μL spore suspension was inoculated into an isotope bottle containing 5 mL of seed medium and cultured in dark at 20 °C and 130 r min^{-1} for 36 h. Afterwards, 1 mL seed broth was inoculated into a 250-mL shake flask containing 50 mL of liquid seed medium. The flask was incubated under the same conditions for 3 days as the first seed. Then the first seed broth was inoculated into 50 mL of liquid seed medium at an inoculation ratio of 10 % (v/v) and cultured under the same conditions to prepare the second seed. For agar plate culture, 200 μL of the second seed broth was spread on the agar medium and incubated at 80 % humidity and 20 °C for 3 days. For submerged fermentation in flask, the second seed broth was inoculated into a 250-mL shake flask containing 75 mL of medium S by 10 % (v/v). Then the strains were cultured in dark at 130 rpm and different temperatures for the desired days. For bioreactor fermentation, 150 mL of the second seed broth was inoculated into a 5-L bioreactor containing 3.5 L of medium S and fermented at 250 rpm and 20 °C for about 14∼21 days. Besides, the *E. coli* strains were incubated in Luria-Bertani medium at 200 rpm and 37 °C for preparation of the required plasmids.

2.2. Construction of plasmids

The plasmids of PFC332 (carrying *CAS9* expression cassette, hph^R) and PFC334 (carrying *CAS9* and sgRNA expression cassette, *ArgB*)[33] were donated by Prof. Reinhard Fischer from the Karlsruhe Institute of Technology, Germany. The pUC19 plasmid was preserved in our laboratory. The primer pair of puc-F1/puc-R1 was used to amplify the sequence of P_{gpdA}-HH-sgRNA-HDV-T_{trpC} from PFC334. This fragment was inserted into the pUC19 plasmid digested with *Eco*RI and *BamH*I to construct the pUC19-sgRNA plasmid. For each gene, different sgRNAs were designed by CHOPCHOP online software. Then two DNA fragments were cloned using primer pairs of inOri F/sgRNA-R and inOri R/sgRNA-F (sgRNA-F and sgRNA-R carry partial sgRNA sequences) (Fig. S2). Then they were fused together by Gibson assembly to form an DNA fragment carrying an intact sgRNA coding sequence linked with a partial plasmid backbone. It was then cloned into pUC19-sgRNA by Gibson assembly. The primer pair of 332-F1/332-R1 was used to amplify the sequence of P_{gpdA}-HH-sgRNA-HDV-T_{trpC} from the pUC19-sgRNA and inserted into PFC332 digested with *Pac*I. Accordingly, the PFC332-sgRNA plasmid was obtained. Afterwards, the upstream and downstream flanking sequences (∼1000 bp) of each target gene were amplified from the genomic DNA of *Geomyces* sp. WNF-15A, respectively, and linked together by overlap-extension PCR. The fused sequence was then assembled into pUC19 digested with *Eco*RI and *BamH*I, generating the donor plasmid. For gene replenishment (knockin), it involved the similar strategies with gene knockout. All the primers used in this study were listed in Table S2.

2.3. Fungal transformation and molecular analysis

The preparation of protoplasts from *Geomyces* sp. WNF-15A and the

PEG-mediated transformation were conducted as previously described [22]. The PFC332-sgRNA plasmid and the donor DNA amplified from the donor plasmid were then co-transformed into the protoplasts to achieve gene editing, and the protoplasts were regenerated by incubation on agar plate (seed medium supplemented with 20 g L^{-1} agar) in dark, and at 80 % humidity and 20 °C for 36–48 h. Afterwards, the upper layer medium was covered using seed medium supplemented with 7.5 g L^{-1} agar and 30 μg mL^{-1} hygromycin B under the same conditions for 5 days. The selected transformants were subjected to spore PCR analysis [22] using the primer pair of Am–F/Am–R to check if the PFC332-sgRNA plasmid was lost. Transformants losing PFC332-sgRNA were collected for genome extraction. Then different primers were designed (Table S1) to validate deficiency of the target genes. Mutants used for phenotype analysis on agar plate or in submerged culture were with target genes completely knocked out.

2.4. Genome sequencing and DEGs detection

The whole genomes of *Geomyces* sp. WNF-15A and the selected mutants (M210, MPS1, MPS3 and MPS4) were sequenced in Shanghai Personalbio Technology Co., Ltd. The whole genome shotgun (WGS) strategy was used to construct libraries with different insert sizes. Then the next-generation sequencing based on the Illumina NovSeq sequencing platform and the third-generation single-molecule sequencing based on the PacBio Sequel sequencing platform were employed to sequence these libraries. The Falcon and CANU softwares were used to assemble the sequencing data from scratch to construct contigs and scaffolds, and the pilon v1.18 software was used to correct the results. The protein-coding genes were predicted using softwares of Augustus (version 3.03), glimmerHMM (version 3.0.1), and GeneMark-ES (version 4.35).

Taking the genome of *Geomyces* sp. WNF-15A as the reference, resequencing was performed to analyze the variants between the mutant strain and the wild-type. The differentially expressed genes (DEGs) were primarily detected by analysis of SNP (single nucleotide polymorphism), Indel (insertion and deletion), SV (chromosomal structural variation), and CNV (copy number variation). Transposon insertions sites or loci with big changes in open reading frames (missing or insertion of large fragments, frameshift mutation) were selected for further analysis. The functional prediction of DEGs includes annotations of NR, KEGG, eggNOG, GO, PHI, Pfam, TCDB, Swissprot and P450 analysis.

2.5. Metabolomics analysis

LC-MS non-targeted metabolomics analysis was involved to analyze global metabolic differences among different strains. Culture samples of 60 h (AGRP production started) and 288 h (AGRP production reached vertex) were analyzed for both the wild-type and mutant strain. Three parallels were analyzed for each sample. Metabolites detection and principal component analysis (PCA) were conducted to evaluate the differences among various samples. Four comparison groups, i.e., wild-type (60 h) *vs.* mutant (60 h), wild-type (288 h) *vs.* mutant (288 h), wild-type (60 h) *vs.* wild-type (288 h), mutant (60 h) *vs.* mutant (288 h), were set for metabolic difference analysis. Fold change <0.5 or >2 and *P*-value <0.05 were identified as differential metabolites. To analyze how the mutant varied cold-adaptive AGRP synthesis at metabolic levels, wild-type (288 h) *vs.* mutant (288 h) were further analyzed. Differential metabolites and their enriched pathway were clarified and analyzed jointly with the genome sequencing results, screening for key genes that affected AGRP production.

2.6. Analytical methods

The AGRP production was quantified by absorbance measurement at 520 nm (OD_{520}) [22,25]. Culture broth of 1 mL was taken periodically and centrifuged at 12,000 rpm for 3 min, and the absorbance value of the diluted supernatant was measured at OD_{520} using a spectrophotometer. The growth of strains was measured by biomass dry weight as described previously [21]. The data were obtained from two or three biological replicates (technical replicates performed if necessary) assayed in duplicate or triplicate, and presented as mean ± S.D. The independent-sample *t*-test was performed to determine the differences among grouped data. Statistical significance was assessed at $P < 0.05$ and $P < 0.01$.

3. Results

3.1. Genome sequencing and annotation of Geomyces sp. WNF-15A

The genome assembly quality of the wild-type *Geomyces* sp. WNF-15A reached high-level as evaluated by BUSCO [33]. As shown in Table 1, we obtained 7,403,461 reads with an N50 length of 2,182,900 bp and the G + C content of 50.08 %. The completeness of the assembly is high as measured by a BUSCO percent completeness score of 99.9 %. The percentage of single-copy genes aligned was achieved as 99.6 %, indicating a good integrity of the genome assembly. The sequencing results were assembled into 61 scaffolds, which were used as the basis for the subsequent genome analysis. We further predicted non-coding RNAs (Table S3) and protein-coding genes (Table S4) throughout the whole genome. As *Geomyces* sp. WNF-15A sequencing had not been reported and it has no closely related genome sequenced strains, we then used multiple databases to jointly annotate its gene functions (Figs. S1–S3). In total, 11,828 protein-coding genes comprising 31,926 exons were obtained, accounting for 52.73 % of the genome size.

3.2. Identification of DEGs by comparative genomic analysis

The mutants of M210, MPS1, MPS3, and MPS4 were preserved as high-quality AGRP producing strains adaptive to normal temperature based on our previous studies [21,22,25]. We thus involved the comparative genomic analysis to identify the mutated sites in these mutants versus to the wild-type. Genome resequencing was performed on these mutants using the wild-type genome as a reference. Resequencing mutation analysis mainly includes detection and annotation of single nucleotide polymorphism (SNP), insertion and deletion (Indel), copy number variation (CNV) and chromosomal variation (SV). The summarized comparative results were shown in Fig. 1. We mainly focused on the analysis of SNPs and Indels which were easily caused by ARTP or transposon insertion. A total of 2309 SNPs were detected, including 1521 transitions and 788 transversions. Further analysis of these SNPs reveals that there were 567 nonsynonymous SNPs that occur in the exon regions, among which 3 of them destroyed the same open reading frame by stopgain (Table 2). Also, 256 Indels were identified, in which the frameshift deletions or insertions that occur in the exon regions were chiefly concerned. Finally, we cleared up 11 mutated genes, comprising 3 stopgains (in the same gene), 3 frameshift insertions, 4 frameshift substitutions and 3 transposon insertions (Table 2). Of note, all the 11 mutated genes encoded hypothetical proteins with predicted or unknown functions.

Table 1
Genome characteristics for the Antarctic fungus *Geomyces* sp. WNF-15A.

genome characteristic	value
Assembly size (bp)	36,898,624
Genes percentage of genome	52.73 %
Complete BUSCOs	99.9 %
G + C content	50.08 %
Protein coding genes	11,828
Average gene length (bp)	1645
Average exons per gene	2.6

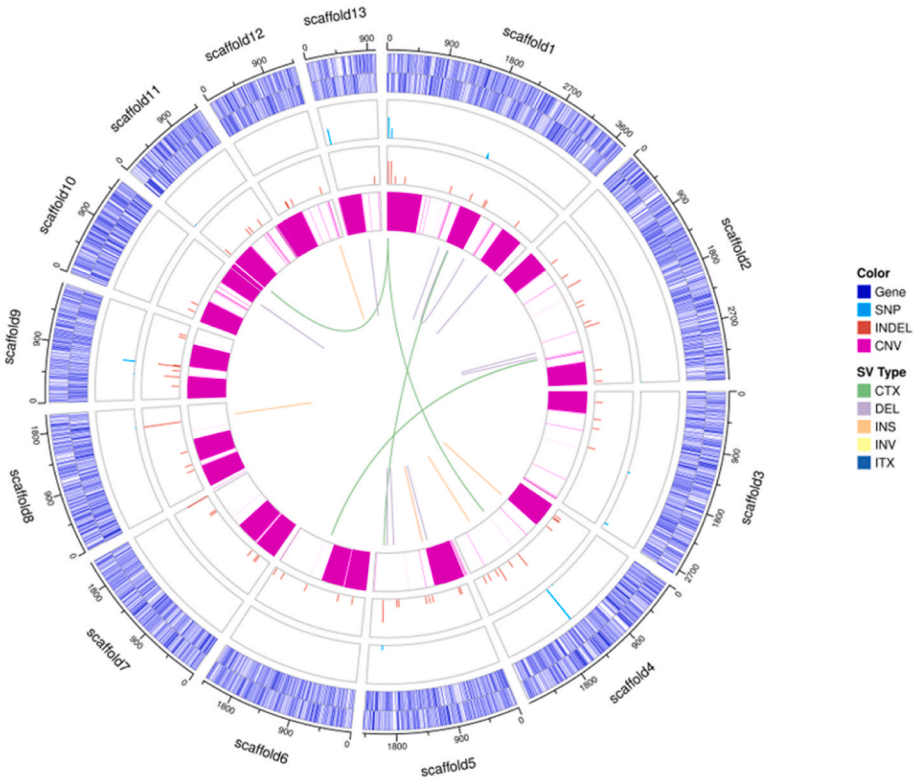

Fig. 1. Circos map described the mutations in the genome of the mutant strains of *Geomyces* sp. WNF-15A. Genomes of four positive mutants (M210, MPS1, MPS3 and MPS4) were re-sequenced and analyzed referring to the assembled genome of the wild-type *Geomyces* sp. WNF-15A. SNP, single nucleotide polymorphism; InDel, insertion and deletion; CNV, copy number variation; SV, structural variation; CTX, inter-chromosomal translocation; DEL, deletion; INS, insertion; INV, inversion; ITX, intra-chromosomal translocation.

Table 2
Differential expressed genes (DEGs) analyzed based on sequencing results.

DEGs	genetic description	function prediction	mutation type
Scaffold4.t481	Hypothetical protein	Unknown	Frameshift insertion
Scaffold3.t910	Hypothetical protein	Cyclic compound binding	SNP (3 stopgains)
Scaffold5.t322	Hypothetical protein	Bio-regulation	Frameshift substitution
Scaffold6.t436	Hypothetical protein	Bio-regulation	Frameshift substitution
Scaffold2.t1133	Hypothetical protein	G protein-coupled receptors	T-DNA insertion
Scaffold2.t134	Hypothetical protein	Membrane transport	T-DNA insertion
Scaffold7.t242	Hypothetical protein	Biological metabolism	Frameshift insertion
Scaffold1.t692	Hypothetical protein	Unknown	T-DNA insertion
Scaffold2.t178	Hypothetical protein	Unknown	Frameshift substitution
Scaffold9.t496	Hypothetical protein	Degradation of drugs	Frameshift insertion
Scaffold2.t704	Hypothetical protein	Unknown	Frameshift substitution

3.3. CRISPR-Cas9 based editing of psychrotrophic candidate genes in wild-type host

To validate the roles of the identified candidate genes in cold-adaptive AGRP synthesis, we need to destroy these genes and evaluate their influence on the fungal phenotypes. However, there was not efficient gene-editing method for the polar *Geomyces* sp. WNF-15A. Thus, we firstly established the marker-free CRISPR-Cas9 gene-editing method in this non-model fungus.

The *CAS9* gene in PFC332 [34] was derived from *Streptococcus pyogenes* and codon-optimized to adapt with filamentous fungi. Previously, we constructed PFC332 derivative plasmids for transposon insertion use in *Geomyces* sp. WNF-15A [22,25], demonstrating the potential of the PFC332 plasmid for gene knockout in this fungus. Therefore, the sgRNA expression cassette from PFC334[33] was cloned and inserted into PFC332, which carries hygromycin resistance gene that functioned in the wild-type *Geomyces* sp. WNF-15A [25]. It generated a plasmid of PFC332-sgRNA, which allows targeted cutting of the candidate genes under the actions of Cas9 and sgRNA. After gene cleavage were implemented, this self-replicating plasmid will be lost when the transformant transferred into a culture without antibiotics. On the other hand, upstream and downstream flanking sequences (~1000 bp) of each candidate gene need to be prepared, which will allow knockout of candidate genes by double-crossover homologous recombination after Cas9-based gene cleavage. Then the pUC19 plasmid backbone was used to load the linked flanking sequences, generating different donor plasmids.

The CRISPR-Cas9 system was then applied for gene editing in *Geomyces* sp. WNF-15A. The amplified PFC332-sgRNA plasmid and linked flanking donor DNA were co-transformed into the host protoplasts to knock out the individual genes (Fig. 2A and Fig. S4). Although the overall knockout efficiency was low, we successfully obtained knockout strains of the 11 candidate genes, which demonstrated that the CRISPR-Cas9 system took effect in this fungus (Fig. 2B). The low efficiency was probably related with the NHEJ repair in genome, which represents the common gene repair pattern in eukaryotic cells. Deficiency of *KU70*, a key gene responsible for the NHEJ, usually improves the efficiency of homologous recombination in cells [35]. Accordingly, we searched a homolog of *Pseudogymnoascus verrucosus* Ku70 (coded by *scaffold6.g724*) of the sequenced *Geomyces* sp. WNF-15A genome and then knocked out

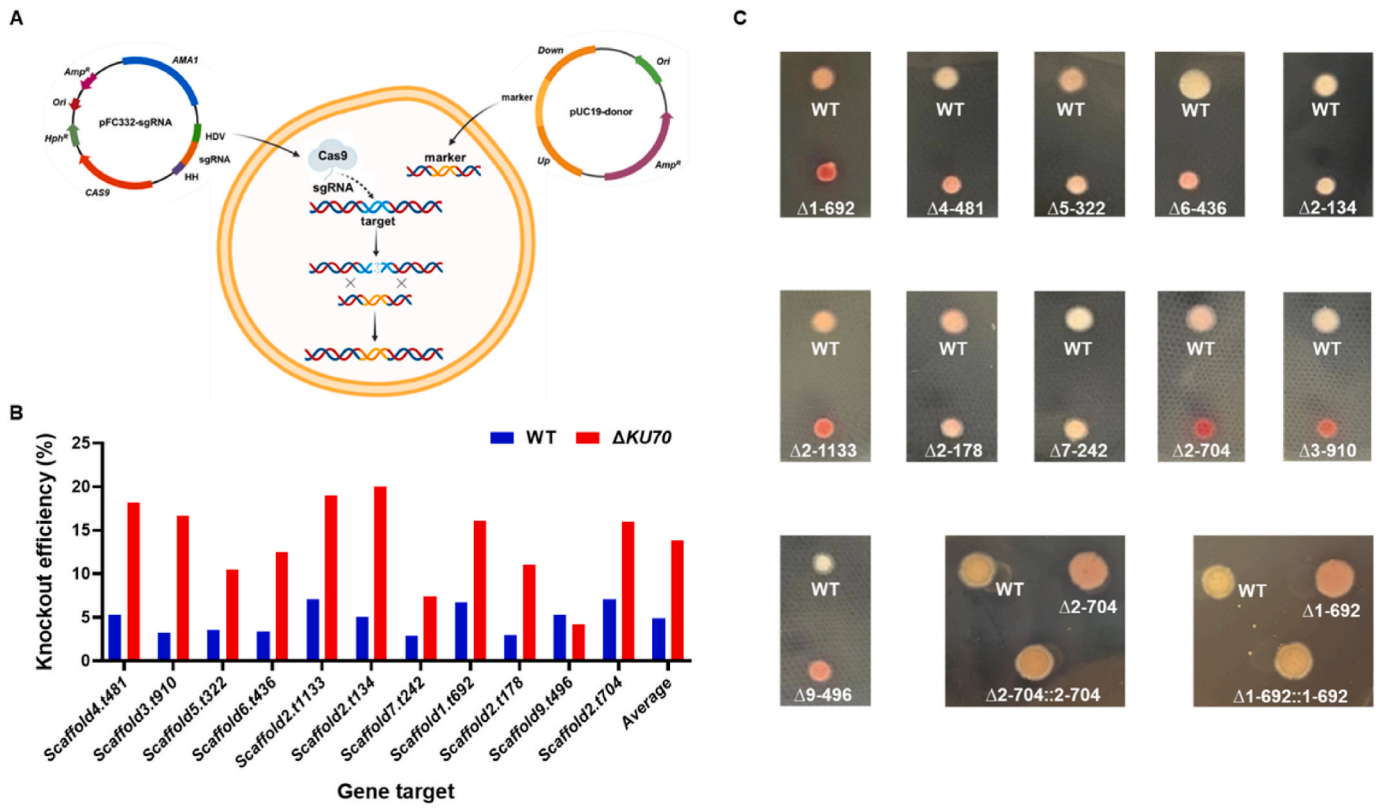

Fig. 2. CRISPR-Cas9 mediated gene knockout and replenishment in *Geomyces* sp. WNF-15A. (A) Scheme for the gene-editing procedure. The details of the pFC332-sgRNA plasmid for expression of sgRNA and Cas9 were shown in Fig. S4. The up and down sequences of the marker gene in pUC19-donor represent the flanking regions of the knockout target gene in the fungal genome. (B) Gene knockout efficiency in Δ*KU70* and wild-type by the developed CRISPR-Cas9 methods. All the candidate genes listed in Table 2 were knocked out for the cold-adaptive AGRP synthesis. Average efficiency of all the tested genes was calculated. Also, the detailed number of total and positive transformants were shown in Table S5 (C) Colony phenotypes of gene knockout strains. Each engineered strain was cultured on a single agar plate at 20 °C for 4–6 days with the wild-type as a control on the same plate. Gene replenishment was performed in Δ1–692 and Δ2–704, which presented the reddest colonies. Submerged culture of the gene replenishment strains in shake flask were also analyzed, which was in accordance with that on agar plate culture.

it by CRISPR-Cas9 system. Deficiency of *KU70* did not affect fungal growth and AGRP production in comparison to the wild-type (Fig. S5). The 11 candidate genes were further knocked out using Δ*KU70* as the parent strain. The knockout efficiency of candidate genes increased obviously as compared to that in the wild-type (Table S5 and Fig. 2B). Finally, the obtained gene-knockout strains were cultured on agar plates at 20 °C to check their functions on AGRP synthesis. Most of the gene-knockout strains showed redder colored colonies comparing with the wild-type (Fig. 2C), revealing their relations with cold-adaptive AGRP synthesis in *Geomyces* sp. WNF-15A. Overall, Δ1–692 and Δ2–704 showed the reddest colonies among all the mutants, thus gene replenishment for each strain was further performed and it recovered the phenotypes in agar plate and shake flask cultures at 20 °C (Fig. 2C and Fig. S6).

3.4. AGRP synthesis by gene knockout strains in submerged cultures

We further tested cell growth and AGRP synthesis of the engineered strains in submerged cultures at different temperatures of 14 °C, 20 °C and 25 °C, respectively. When cultured in shake flask at 14 °C, the mutants of Δ4–481, Δ3–910, Δ2–134, Δ1–692, Δ9–496 and Δ2–704 showed increased production of AGRP compared with the wild-type, while biomass dry weight for all strains showed not big differences. Among them, the production of AGRP by Δ2–704 reached the highest level (OD_{520} = 41.9), which was 140 % higher than the wild-type (Fig. 3A and Fig. S7). When cultured at 20 °C, the production of AGRP reduced obviously for each strain in comparison to 14 °C. Nevertheless, the mutants of Δ4–481, Δ3–910, Δ2–1133, Δ1–692, Δ2–178, and Δ2–704 still showed increased production of AGRP compared to the wild-type. Of note, the AGRP production by Δ1–692 (OD_{520} = 17.7) and Δ2–704 (OD_{520} = 18.6) increased by 156 % and 169 %, respectively, comparing with the wild-type (Fig. 3B and Fig. S8). Moreover, the AGRP synthetic capacity by Δ1–692 and Δ2–704 at 20 °C reached comparable to the wild-type at 14 °C (Fig. 3A and B). Besides, the biomass dry weight differed not that much among various mutants. When temperature increased to 25 °C, the wild-type strain nearly ceased AGRP synthesis, while Δ4–481, Δ3–910, Δ1–692, Δ2–178, Δ9–496, and Δ2–704 produced higher levels of AGRP than the wild-type. Among them, Δ1–692 represented the most dominant producing strains (Fig. 3C and Fig. S9). Generally, cell growth of each strain including the wild-type turned to be slow as compared to that at 14 °C and 20 °C.

Then Δ1–692 and Δ2–704 were used as the starting hosts for combinatorial knockout of the candidate genes regarding cold-adaptive AGRP synthesis. However, it was not easy to knock out these genes combinatorially. Finally, five double-gene knockout strains (Δ2–704Δ1-692, Δ2–704Δ4-481, Δ2–704Δ2-134, Δ2–704Δ9-496, Δ2–704Δ7-242) and one triple-gene knockout strain (Δ2–704Δ4-481Δ2–178) were obtained. It seemed that some double knockout strains showed obvious AGRP production increase at 14 °C and 20 °C, but the improved level was limited especially when culture at 25 °C (Fig. 3D–F, Figs. S10–S12). Besides, the triple-gene knockout strain severely damaged cell growth and changed fungal morphology (abnormal flocculent biomass in flask, data not shown), which resulted in almost no AGRP production.

As the engineered strains of Δ1–692 and Δ2–704 demonstrated good production of AGRP under normal temperatures, we then evaluated their actual AGRP synthetic capacity in bioreactor. Cultured in 5-L

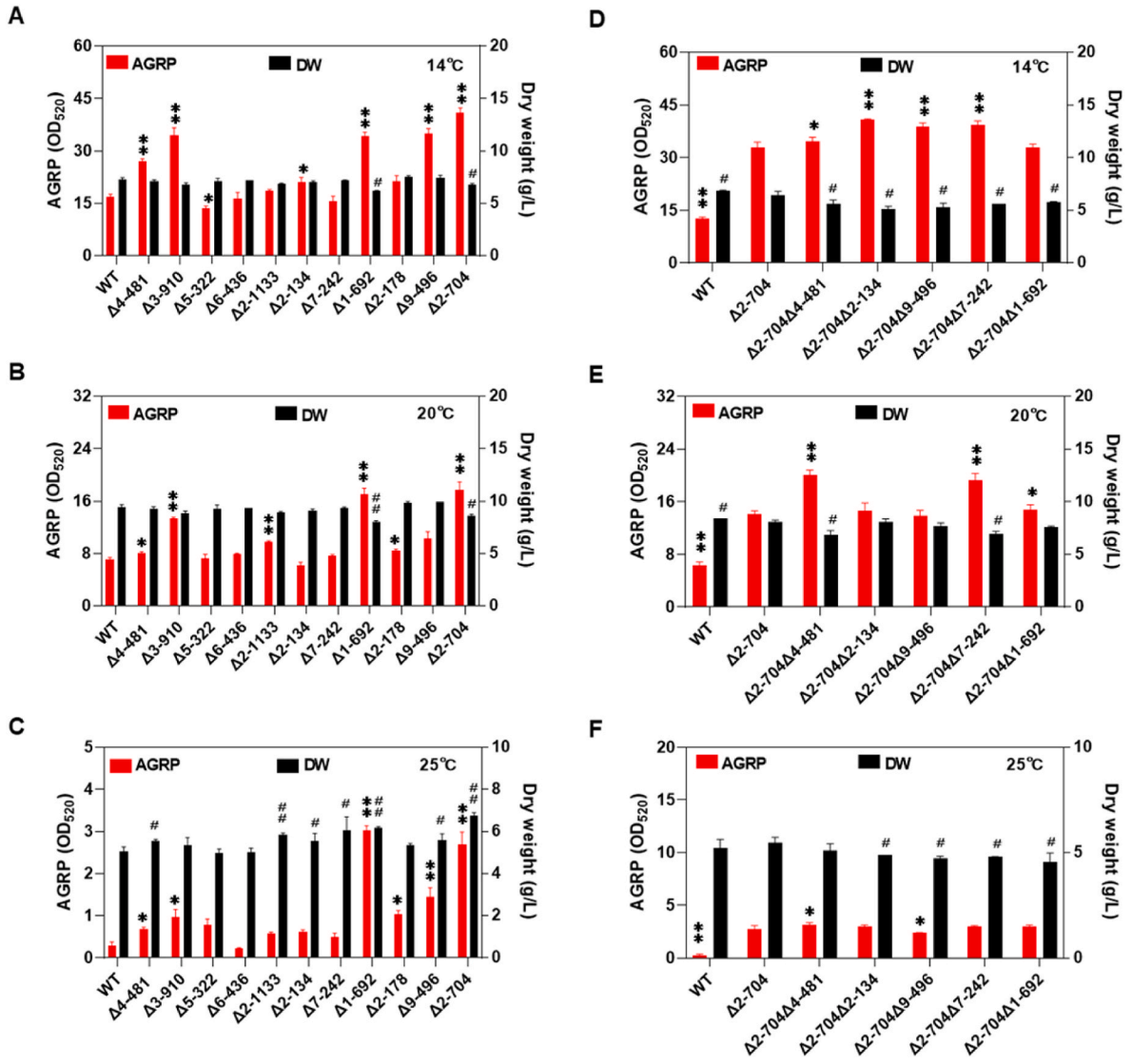

Fig. 3. AGRP production and biomass growth of gene knockout strains. (Ã C) Single-gene knockout strains were cultured at temperatures of 14 °C, 20 °Cand 25 °C. (E ~ F) Double-gene knockout strains were cultured at temperatures of 14 °C, 20 °C and 25 °C. The statistical significance of AGRP and DW of each single-gene knockout strain is shown relative to the wild-type, and the statistical significance of AGRP and DW of each double-gene knockout strain is shown relative to Δ2–704. $^{\#\#}P < 0.01$, $^{\#}P < 0.05$ for DW; $^{**}P < 0.01$, $^{*}P < 0.05$ for AGRP; the column without marker means not significance. The error bars represent the standard deviation of different biological replicates (with two or three technical replicates) assayed in duplicate or triplicate. Time profiles of AGRP production and biomass growth of different strains related to this figure were shown in Figs. S7–S12.

parallel bioreactors, all the strains including Δ1–692, Δ2–704 and the wild-type produced much more AGRP than that in shake flask under the same temperature (Fig. 4). At 20 °C, the highest level of AGRP for each strain was achieved after 13–14 days culture. The AGRP productions from Δ1–692 (OD_{520} of 27.9) and Δ2–704 (OD_{520} of 26.7) reached nearly 2-fold of the wild-type (OD_{520} of 14.7) (Fig. 4A–C).

Cell growth of Δ1–692 and Δ2–704 was a bit weaker than that of the wild-type. Besides, the broth pH changed smoothly and similarly among all the three strains (Fig. 4A–C). Generally, the AGRP productions by the engineered strains at 20 °C were comparable to that by the wild-type at 14 °C (Fig. 4D). When cultured at 25 °C, the wild-type was almost unable to produce AGRP in bioreactor, but the Δ1–692 (OD_{520} of 6.4) and Δ2–704 (OD_{520} of 6.2) broke this limit and produced AGRP successfully (Fig. 4E–F). Cell growth and pH variations kept almost synchronously between the two strains. Also, AGRP synthetic period extended severely at 25 °C for both strains. It reached the highest levels after 17–18 days culture and maintained stable until the culture endpoint at 23 days (Fig. 4E–F).

3.5. *Comparative metabolomic analysis of the wild-type and Δ1–692 mutant*

LC-MS non-targeted metabolomics analysis was further performed on the Δ1–692 and the wild-type, given that Δ1–692 produced the highest level of AGRP at 20 °C and 25 °C (Fig. 3). Also, gene size of *scaffold1.t692* was small (Table S6), which was more likely an upstream regulatory gene. To investigate metabolic differences between different strains at different times, we selected samples from AGRP early production phase (60 h) and high production phase (288 h) of both the Δ1–692 and the wild-type at 20 °C for metabolomics analysis. There were 589 differential metabolites between the wild-type and Δ1–692 at 60 h culture and 557 differential metabolites at 288 h culture, sharing 218 differential metabolites in both stages (Fig. S13). On the other hand, 924 differential metabolites were identified between 60 h and 288 h cultures of the wild-type, but only 265 differential metabolites were identified between 60 h and 288 h cultures of the Δ1–692 (137 metabolites in common), indicating deficiency of *scaffold1.t692* greatly

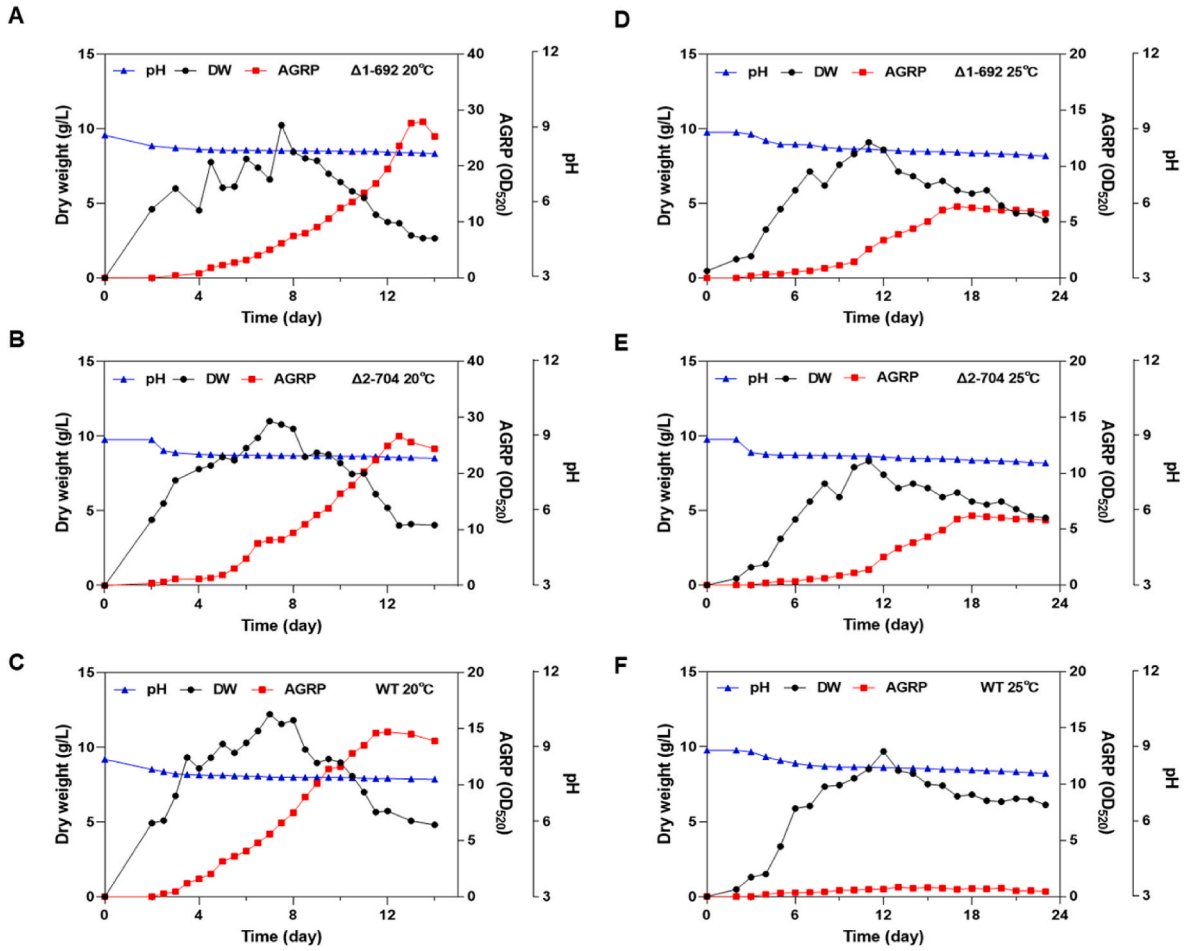

Fig. 4. Time profiles of Δ1–692 and Δ2–704 fermented at normal temperature in 5-L bioreactors. (A) Δ1–692 at 20 °C; (B) Δ2–704 at 20 °C; (C) wild-type at 25 °C; (D) Δ1–692 at 25 °C; (E) Δ2–704 at 25 °C; (F) wild-type at 25 °C. Fermentation process control is described in methods.

changed cell metabolism (Fig. S13). Totally, 33 differential metabolites were shared by all the four groups, most of which were organic acids, amino acids and secondary metabolites.

To clarify the increased AGRP synthesis of the Δ1–692 in comparison to the wild-type, we then focused on their differential metabolites in the high production phase (288 h). The detected metabolites were mainly composed of organic acids, amino acids, lipids, aromatic compounds, and different kinds of secondary metabolites (Fig. S14). The 557 differential metabolites of the detected metabolites in this group (Fig. S13) were classified and mapped to KEGG pathways (Fig. 5A). The results revealed that the differential metabolites enriched in nucleotide and amino acids metabolism, sulfur relay systems, membrane transport processes, secondary metabolite synthesis, etc. (Fig. 5A and B). Among all the 557 differential metabolites, we selected 8 metabolites with big changes and high-level content. Accordingly, 8 upstream candidate genes for the synthesis of these metabolites were identified based on the metabolomic and genomic data (Table 3).

3.6. Functional analysis of the candidate genes from metabolomic analysis

The identified 8 genes of metabolic pathways (Fig. 6A) were knocked out in the wild-type, and the obtained engineering strains were investigated under different temperatures. The AGRP synthesis was generally improved in the strains of Δ8-432 and Δ20-56 (Fig. 6B–D and Figs. S15–S17). The omics data showed that *scaffold8.t432* and *scaffold20.t56* coded for key enzymes functioned in the biosynthetic pathways of flavonoids and other secondary metabolites, respectively (Table 3). Knockout of them may weaken the competitive pathways and in turn improve AGRP synthesis via polyketides pathway [21]. We also knocked out these genes in Δ1-692 to test whether overlay gene deficiency will facilitate AGRP synthesis further. Knockout of *scaffold8.t432* or *scaffold20.t56* could almost not improve AGRP synthesis comparing with the parent strain of Δ1-692 (Fig. 6E–G and Figs. S18–S20), which was different from that in the wild-type. Generally, knockout of genes related with amino acids and lipid metabolism was adverse to the AGRP synthesis. Deficiency of *scaffold3.t755*, a gene related with starch metabolism, decreased AGRP synthesis and cell growth in both wild-type and Δ1-692. It probably ascribed to that the mycelial cells cultured in the medium with starch as the main carbon source. Instead, deficiency of other genes but not *scaffold3.t755* affected cell growth not severely.

4. Discussion

Microorganisms inhabiting in polar regions often show special physiological characteristics and produce various substances with unique structures and functions. These products showed promising outlooks for the potential use in industrial areas of food, drugs, cosmetics, and so on.[19] However, their special physiological traits may also bring many difficulties in the large-scale culture. Take cold adaptation as an example, the cold temperature control, poor mass transfer at low temperature, slow cell growth and long culture phase make it high-cost and hard process control for the potential industrialization. The polar fungus *Geomyces* sp. WNF-15A is such kind of psychrotrophic strain. It produces a promising pigment AGRP that could be used in food and

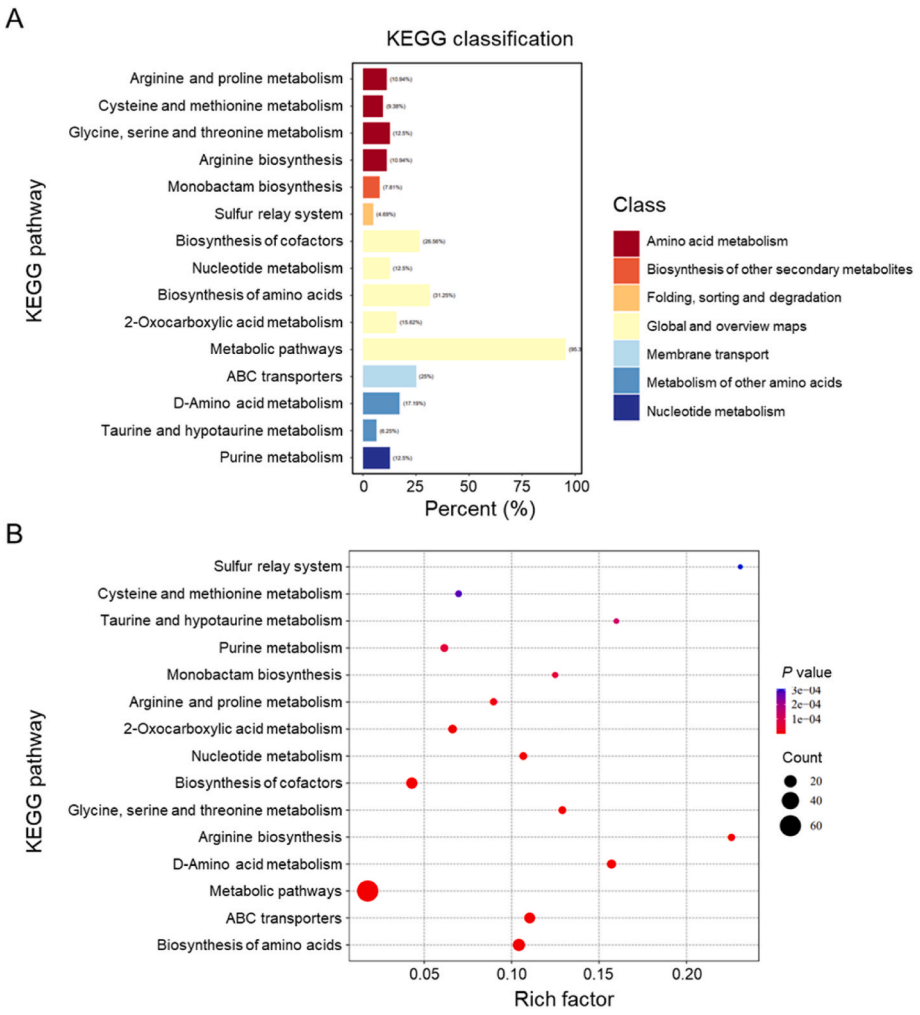

Fig. 5. KEGG analysis of differential metabolites between Δ1-692 (288 h culture) and wild-type (288 h culture). (A) KEGG classification map of differential metabolites. The percentage of annotated differential metabolites in each pathway to all annotated differential metabolites are shown. Metabolic pathways with similar functions are represented by the same color. (B) KEGG enrichment map of differential metabolites. Number of differential metabolites annotated in a certain pathway relative to the total compounds in the same pathway was shown. These differential genes were identified from the total up- and down-regulated genes (Fig. S14) by fold-change value (<0.5 or >2) and *P*-value <0.05.

Table 3
Analyze the upstream genes of the differential metabolites.

differential metabolite	upstream gene	genetic description	metabolic pathways
3-Hydroxy-3-methylglutaryl-CoA	*Scaffold9.t263*	hydroxymethylglutaryl-CoA synthase (HMGCS)	Amino acid metabolism
Pinocembrin chalcone	*Scaffold8.t432*	chalcone synthase (CHS)	Flavonoid biosynthesis
Zeaxanthin	*Scaffold5.t195*	Zeaxanthin epoxidase (ABA1 or ZEP)	Carotenoid biosynthesis
Crotonoyl-CoA	*Scaffold10.t441*	glutaryl-CoA dehydrogenase (GDH)	Lysine degradation
2-(p-Hydroxyphenyl) ethylamine	*Scaffold6.t587*	l-DOPA/tyrosine decarboxylase (DDC/TDC)	Tyrosine metabolism
dTDP-4-oxo-6-deoxy-d-glucose	*Scaffold20.t56*	dTDP-glucose 4,6-dehydratase (rfbB)	Biosynthesis of other secondary metabolites
alpha-d-Glucose 1-phosphate	*Scaffold3.t755*	Glycogen phosphorylase (PYG)	Starch and sucrose metabolism
Methylmalonate	*Scaffold5.t501*	aldehyde dehydrogenase (ALDH)	PPAR signaling pathway

cosmetics, but the cold-adaptive AGRP production behavior severely limited its fermentation scale-up. Recently, our group has attempted to screen normal temperature-adaptive AGRP producing strains by strategies of physical mutation [21] and transposons insertion mutation [22,25]. As a result, a series of mutants realized high-level AGRP production at 20 °C and several ones even broke the bottleneck of production repressed at 25 °C in the wild-type. For all that, the mutated sites in the genome still remained unknown.

In this study, with the comparative genomic analysis of the wild-type and mutant strains, we successfully identified 11 candidate genes that might be related with cold-adaptive AGRP synthesis from 2309 SNPs and 256 Indels. It is noteworthy that all these 11 candidate genes encoded hypothetical proteins with low-identity predicted or absolutely unknown functions. To validate their roles, we need to destroy the genes and evaluate the changes of cold-adaptive AGRP synthesis by this strain. We firstly established a CRISPR-Cas9 guided gene editing system for this fungus, but the editing efficiency was not high even in an NHEJ-deficient Δ*KU70* strain. It might be related with the physiological characteristics of *Geomyces* sp. WNF-15A and needs further optimization to increase the editing efficiency. Genetic manipulation tools are often limited in filamentous fungi especially the isolated wild-type strains of antibiotic insensitivity and multicellular nucleus, even with today's advanced CRISPR-Cas9 editing techniques. Nevertheless, we finally

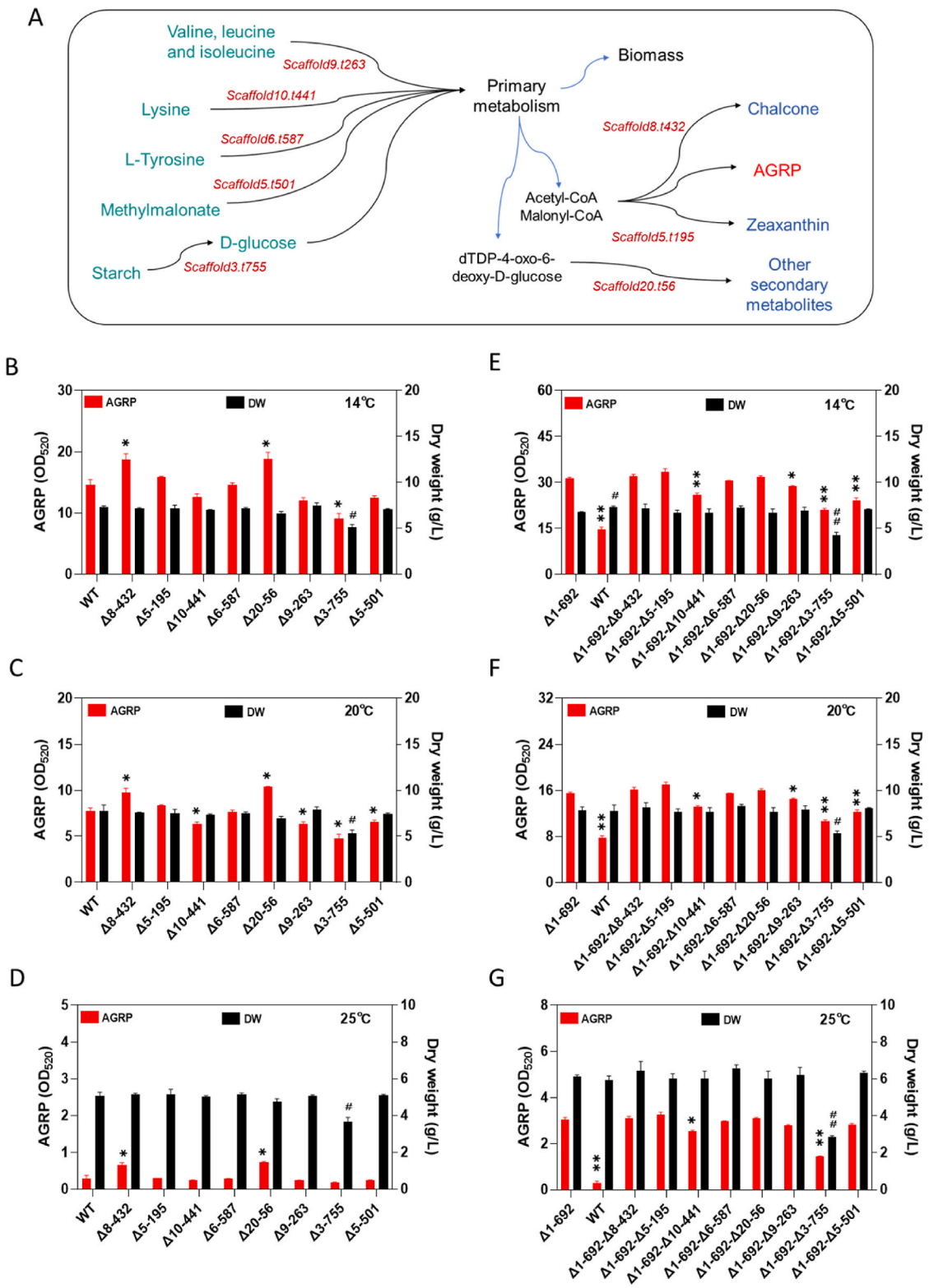

Fig. 6. AGRP production and biomass growth of strains with metabolic gene knockout from the wild-type and Δ1–692. (A) Predicted roles of the metabolic related differential genes from Table 3 in primary and secondary metabolism. (B ~ D) Genes were knocked out from the wild-type and cultured at temperatures of 14 °C, 20 °Cand 25 °C. (E ~ G) Genes were knocked out from Δ1–692 and cultured at temperatures of 14 °C, 20 °C and 25 °C. The statistical significance of AGRP and DW of each single-gene knockout strain is shown relative to the wild-type, and the statistical significance of AGRP and DW of each double-gene knockout strain is shown relative to Δ1–296. $^{\#\#}P < 0.01$, $^{\#}P < 0.05$ for DW; $^{**}P < 0.01$, $^{*}P < 0.05$ for AGRP; the column without marker means not significance. The error bars represent the standard deviation of different biological replicates (with two or three technical replicates) assayed in duplicate or triplicate. Time profiles of AGRP production and biomass growth of different strains related to this figure were shown in Figs. S15–S20.

knocked out all the 11 genes in the *Geomyces* sp. WNF-15A and verified their roles in regulation of cold-adaptive AGRP synthesis.

Of note, knockout of *scaffold1.692* (Δ1-692) and *scaffold2.t704* (Δ2-704) highly improved AGRP synthesis at all the tested temperatures. Gene replenishment recovered their phenotype and further validated their functions. In particular, AGRP productions by Δ1-692 and Δ2-704 at 20 °C were comparable to that by the wild-type at 14 °C. The two strains also produced AGRP effectively at 25 °C, which broke the bottleneck of almost non-production in the wild-type under the same temperature. The unlocked normal temperature-adaptive AGRP synthesis was also verified in bioreactor scale, and the production levels even reached two-fold of that in flask culture. These results revealed that *scaffold1.692* and *scaffold2.t704* play important roles in regulation of cold-adaptive AGRP synthesis in this fungus. Double-gene knockout was also investigated in the Δ2-704 and Δ1-692. However, limited genes were successfully knocked out in the Δ2-704, for which only the Δ2–704Δ4-481 and Δ2–704Δ9-496 slightly improved AGRP synthesis as compared to the Δ2-704 at 25 °C. Besides, only one triple-gene knockout strain Δ2–704Δ4-481Δ2–178 was obtained, which showed bad growth and undetected AGRP production. In addition, we were not able to obtain any double-gene knockout strain using Δ1-692 as the parent host, even with several rounds of gene-knockout experiments. Thus deletion of these genes in the Δ1–692 might be unfavorable to the fungus. Generally, combinatorial knockout of the psychrotrophic candidate genes based on the Δ2-704 or Δ1-692 seemed not a preferred strategy for the purpose of constructing normal temperature-adaptive AGRP producing strains in this study. Nevertheless, it is worth developing other knockdown or improved knockout strategies to obtain desired mutants and clarify the functional relationship among these psychrotrophic candidate genes in the near future. To present, although cold-adaptive mechanisms have been reported in bacteria, *e.g.*, cryptic prophage excision, cell membrane adaptation, RNA metabolism adaptation, etc. [36,37], they are seldom reported in fungi especially those from polar regions. Therefore, the Antarctic *Geomyces* sp. WNF-15A may have some unknown regulatory mechanisms to make it adapt to the cold environment. Future studies on the molecular regulation steps with these genes may help reveal the underneath mechanisms of cold-adaptive AGRP synthesis in this strain. Besides, some cold-adaptive genes can be searched from the genome data of psychrotrophic *Pseudogymnoascus* sp., which can cause white-nose syndrome (WNS) in many bat species [38]. These cold-adaptive genes might also provide targets for the investigation of pathogenic mechanisms of psychrotrophic fungi.

Comparative metabolomic analysis were performed between the Δ1-692 and the wild-type to track differential cell metabolism related with AGRP synthesis. Knockout of *scaffold1.692* leads to remarkable differences in the metabolism of amino acids, organic acids, nucleotides, as well as secondary metabolites in comparison to the wild-type. The results indicated that AGRP reached higher production in Δ1-692 by regulation of global metabolic pathways, especially downregulation of the competitive pathways. We thus figured out metabolites with large differences in detected levels and metabolic pathways with a large proportion of differential metabolites. The upstream genes for the key metabolites or pathways were selected and knocked out, which indeed facilitated AGRP production in the wild-type. However, how the *scaffold1.692* regulates the variations of these metabolic pathways remains unknown. We cannot obtain its function annotations from any database, and so was the *scaffold2.t704* (detailed sequences in Table S6). Therefore, they may represent new regulatory genes in fungal cold-adaptive mechanisms. In future, transcriptome analysis can be performed to identify targets regulated by *scaffold1.692* and *scaffold2.t704*, which may provide clues for the signal transduction decoding of cold-adaptive AGRP synthesis in *Geomyces* sp. WNF-15A.

As for the AGRP production, it achieved a highly increased level at 20 °C, but the fermentation process may be further improved by precursor and pH control, substrate feeding strategies, morphology regulation, and so on. Although we have broken the limit of cold dependent synthesis of AGRP by the wild-type at 25 °C, the actual AGRP production was still low as compared to that at 20 °C. Future cold-adaptation signal transduction clarification, systematic genetic modification and fermentation optimization are needed to improve AGRP production under the conditions of the industrial application scenes.

5. Conclusion

Genes related with cold-adaptive AGRP synthesis by polar psychrotrophic fungus were identified by comparative omics analysis. Deficiency of *scaffold2.t704* and *scaffold1.t692* with unknown functions highly improved AGRP synthesis and broke the normal-temperature repression on AGRP synthesis. *Scaffold1.t692* affected AGRP production by regulating the global metabolic pathways including the competitive pathways of AGRP. This study provides new references for exploitation and utilization of psychrotrophic fungal resources.

Data availability

Original data of genomic and metabolomic sequencing may be required from the corresponding authors for only academic studies. Other data generated or analyzed during this study are included in this article.

Ethical approval and informed consent

We declare that this paper does not report any data collected from humans or animals.

CRediT authorship contribution statement

Haoyu Long: Data curation, Formal analysis, Writing – original draft. **Jiawei Zhou:** Data curation, Formal analysis. **Yanna Ren:** Formal analysis. **Jian Lu:** Formal analysis. **Nengfei Wang:** Resources. **Haifeng Liu:** Writing – review & editing. **Xiangshan Zhou:** Writing – review & editing. **Menghao Cai:** Conceptualization, Data curation, Formal analysis, Funding acquisition, Project administration, Writing – original draft, Writing – review & editing.

Declaration of competing interest

The authors declare that they have no known competing financial interests or personal relationships that could have appeared to influence the work reported in this paper.

Acknowledgements

This study was supported by the National Natural Science Foundation of China (42176238) and the 111 Project of China (B18022). We thank Shanghai Personalbio Technology Co., Ltd. for the support of genome sequencing, and Shanghai Sangon Biotech Co., Ltd. for the support of metabolome sequencing.

Appendix A. Supplementary data

Supplementary data to this article can be found online at https://doi.org/10.1016/j.synbio.2024.07.002.

References

[1] Hayward MK, Dewey ED, Shafer KN, Huntington AM, Burchell BM, Stokes LM, et al. Cultivation and characterization of snowbound microorganisms from the South Pole. Extremophiles 2021;25:159–72. https://doi.org/10.1007/s00792-021-01218-z.

[2] Liu S, Fang S, Cong B, Li T, Yi D, Zhang Z, et al. The Antarctic moss pohlia nutans genome provides insights into the evolution of Bryophytes and the adaptation to

extreme terrestrial habitats. Front Plant Sci 2022;13:920138. https://doi.org/10.3389/fpls.2022.920138.
[3] Cassaro A, Pacelli C, Aureli L, Catanzaro I, Leo P, Onofri S. Antarctica as a reservoir of planetary analogue environments. Extremophiles 2021;25:437–58. https://doi.org/10.1007/s00792-021-01245-w.
[4] Rosa LH, Zani CL, Cantrell CL, Duke SO, Rosa CA. Fungi in Antarctica: diversity ecology effects of climate change and bioprospection for bioactive compounds. ROSA L H Fungi of Antarctica: diversity ecology and biotechnological applications. Cham: Springer International Publishing; 2019. p. 1–17. https://doi.org/10.1007/978-3-030-18367-7_1.
[5] Brunati M, Rojas JL, Sponga F, Ciciliato I, Losi D, Göttlich E, et al. Diversity and pharmaceutical screening of fungi from benthic mats of Antarctic lakes. Mar Genomics 2009;2(1):43–50. https://doi.org/10.1016/j.margen.2009.04.002.
[6] Carvalho CR, Gonçalves VN, Pereira CB, Johann S, Galliza IV, Alves TMA, et al. The diversity antimicrobial and anticancer activity of endophytic fungi associated with the medicinal plant Stryphnodendron adstringens (Mart.) Coville (Fabaceae) from the *Brazilian savannah*. Symbiosis 2012;57(2):95–107. https://doi.org/10.1007/s13199-012-0182-2.
[7] Gonçalves VN, Carvalho CR, Johann S, Mendes G, Alves TMA, Zani CL, et al. Antibacterial, antifungal and antiprotozoal activities of fungal communities present in different substrates from Antarctica. Polar Biol 2015;38(8):1143–52. https://doi.org/10.1007/s00300-015-1672-5.
[8] Li Y, Sun B, Liu S, Jiang L, Liu X, Zhang H, Che Y. Bioactive asterric acid derivatives from the Antarctic ascomycete fungus *Geomyces* sp. J Nat Prod 2008;71:1643–6. https://doi.org/10.1021/np8003003.
[9] Purić J, Vieira G, Cavalca LB, Sette LD, Ferreira H, Vieira MLC, et al. Activity of Antarctic fungi extracts against phytopathogenic bacteria. Lett Appl Microbiol 2018;66(6):530–6. https://doi.org/10.1111/lam.12875.
[10] Santiago IF, Alves TM, Rabello A, Sales Junior PA, Romanha AJ, Zani CL, et al. Leishmanicidal and antitumoral activities of endophytic fungi associated with the Antarctic angiosperms *Deschampsia antarctica Desv.* and *Colobanthus quitensis (Kunth) Bartl.* Extremophiles 2012;16(1):95–103.
[11] Vieira G, Purić J, Morão LG, Dos Santos JA, Inforsato FJ, Sette LD, Ferreira H, et al. Terrestrial and marine Antarctic fungi extracts active against *Xanthomonas citri subsp. citri*. Lett Appl Microbiol 2018;67(1):64–71. https://doi.org/10.1111/lam.12890.
[12] Wu G, Ma H, Zhu T, Li J, Gu Q, Li D. Penilactones A and B, two novel polyketides from Antarctic deep-sea derived fungus *Penicillium crustosum* PRB-2. Tetrahedron 2012;68(47):9745. https://doi.org/10.1016/j.tet.2012.09.038. 9549.
[13] Baskaran A, Kaari M, Venugopal G, Manikkam R, Joseph J, Bhaskar PV. Anti freeze proteins (Afp): properties, sources and applications - a review. Int J Biol Macromol 2021;189:292–305. https://doi.org/10.1016/j.ijbiomac.2021.08.105.
[14] Cavalcante SB, Dos Santos Biscaino C, Kreusch MG, da Silva AF, Duarte RTD, Robl D. The hidden rainbow: the extensive biotechnological potential of Antarctic fungi pigments. Braz J Microbiol 2023;54:1675–87. https://doi.org/10.1007/s42770-023-01011-4.
[15] de Menezes GC, Godinho VM, Porto BA, Gonçalves VN, Rosa LH. *Antarctomyces pellizariae* sp. nov a new endemic blue snow resident psychrophilic ascomycete fungus from Antarctica. Extremophiles 2017;21(2):259–69. https://doi.org/10.1007/s00792-016-0895-x.
[16] Núñez-Pons L, Avila C, Romano G, Verde C, Giordano D. UV-Protective compounds in marine organisms from the southern ocean. Mar Drugs 2018;16(9):336. https://doi.org/10.3390/md16090336.
[17] Tsuji M, Yokota Y, Shimohara K, Kudoh S, Hoshino T. An application of wastewater treatment in a cold environment and stable lipase production of Antarctic basidiomycetous yeast *Mrakia blollopis*. PLoS One 2013;8:e59376. https://doi.org/10.1371/journal.pone.0059376.
[18] Zucconi L, Canini F, Temporiti ME, Tosi S. Extracellular enzymes and bioactive compounds from Antarctic terrestrial fungi for bioprospecting. Int J Environ Res Publ Health 2020;17(18):6459. https://doi.org/10.3390/ijerph17186459.
[19] Furbino LE, Godinho VM, Santiago IF, Pellizari FM, Alves TM, Zani CL, et al. Diversity patterns ecology and biological activities of fungal communities associated with the endemic macroalgae across the Antarctic peninsula. Microb Ecol 2014;67(4):775–87. https://doi.org/10.1007/s00248-014-0374-9.
[20] Wang NF, Zhao Q, Zhang P. Antarctic fungus coloring compound. Patent. People's Republic of China: CN 104804007 a. 2015.07.29.
[21] Huang HZ, Ding LL, Lu J, Wang NF, Cai MH. Combinatorial strategies for production improvement of red pigment from Antarctic fungus *Geomyces* sp. J Food Sci 2020;85:3061–71. https://doi.org/10.1111/1750-3841.15443.
[22] Ding L, Huang H, Lu F, Lu J, Zhou X, Zhang Y, et al. Transposon insertion mutation of Antarctic psychrotrophic fungus for red pigment production adaptive to normal temperature. J Ind Microbiol Biotechnol 2021;49(1):kuab073. https://doi.org/10.1093/jimb/kuab073.
[23] Jin BB, Wang NF, Zhang M, Zhao Q, Zuo-Hao W, Wang YB, et al. The stability comparison of Antarctic red pigment and cochineal pigment. Food Ferment Ind 2014;40(2):164–9. https://doi.org/10.13995/j.cnki.11-1802/ts.2014.02.043.
[24] Wang FQ, Xu B, Sun YF, Zang JY, Li XM, Wang NF. Identification of an Antarctic fungus and property analysis of its secretory pigment. J Chin Inst Food Sci Technol 2013;13(3):189–95. https://doi.org/10.16429/j.1009-7848.2013.03.035.
[25] Lu F, Ren Y, Ding L, Lu J, Zhou X, Liu H, et al. Minos and Restless transposon insertion mutagenesis of psychrotrophic fungus for red pigment synthesis adaptive to normal temperature. Bioresourc Bioproc 2022;9:1–11. https://doi.org/10.1186/s40643-022-00622-3.
[26] AbuSara NF, Piercey BM, Moore MA, Shaikh AA, Nothias LF, Srivastava SK, et al. Comparative genomics and metabolomics analyses of clavulanic acid-producing *Streptomyces* species provides insight into specialized metabolism. Front Microbiol 2019;10:2550. https://doi.org/10.3389/fmicb.2019.02550.
[27] Chiteri KO, Rairdin A, Sandhu K, Redsun S, Farmer A, O'Rourke JA, et al. Combining GWAS and comparative genomics to fine map candidate genes for days to flowering in mung bean. BMC Genom 2024;25(1):270. https://doi.org/10.1186/s12864-024-10156-x.
[28] Liu C, Gao J, Cui X, Li Z, Chen L, Yuan Y, et al. A towering genome: experimentally validated adaptations to high blood pressure and extreme stature in the giraffe. Sci Adv 2021;7(12):eabe9459. https://doi.org/10.1126/sciadv.abe9459.
[29] Wang C, Lu J, Sha X, Qiu Y, Chen H, Yu Z. TRPV1 regulates ApoE4-disrupted intracellular lipid homeostasis and decreases synaptic phagocytosis by microglia. Exp Mol Med 2023;5(2):347–63. https://doi.org/10.1038/s12276-023-00935-z.
[30] Zha W, You A. Comparative iTRAQ proteomic profiling of proteins associated with the adaptation of brown planthopper to moderately resistant vs. susceptible rice varieties. PLoS One 2020;15:e0238549. https://doi.org/10.1371/journal.pone.0238549.
[31] Bailey JE, Sburlati A, Hatzimanikatis V, Lee K, Renner WA, Tsai PS. Inverse metabolic engineering: a strategy for directed genetic engineering of useful phenotypes. Biotechnol Bioeng 2002;79(5):568–79. https://doi.org/10.1002/bit.10441.
[32] Huang M, Bao J, Hallström BM, Petranovic D, Nielsen J. Efficient protein production by yeast requires global tuning of metabolism. Nat Commun 2017;8:1131. https://doi.org/10.1038/s41467-017-00999-2.
[33] Simão FA, Waterhouse RM, Ioannidis P, Kriventseva EV, Zdobnov EM. BUSCO: assessing genome assembly and annotation completeness with single-copy orthologs. Bioinformatics 2015;231(19):3210–2. https://doi.org/10.1093/bioinformatics/btv351.
[34] Nodvig CS, Nielsen JB, Kogle ME, Mortensen UH. A CRISPR-Cas9 system for genetic engineering of flamentous fungi. PLoS One 2015;10(7):e0133085. https://doi.org/10.1371/journal.pone.0133085.
[35] Liu Q, Shi X, Song L, Liu H, Zhou X, Wang Q, et al. CRISPR-Cas9-mediated genomic multiloci integration in *Pichia pastoris*. Microb Cell Factories 2019;218(1):144.
[36] Barria C, Malecki M, Arraiano CM. Bacterial adaptation to cold. Microbiology 2013;159(112):2437–43. https://doi.org/10.1099/mic.0.052209-0.
[37] Zeng Z, Liu X, Yao J, Guo Y, Li B, Li Y, et al. Cold adaptation regulated by cryptic prophage excision in *Shewanella oneidensis*. ISME J 2016;10(12):2787–800. https://doi.org/10.1038/ismej.2016.85.
[38] Zukal J, Bandouchova H, Bartonicka T, Berkova H, Brack V, Brichta J, et al. White-nose syndrome fungus: a generalist pathogen of hibernating bats. PLoS One 2014;9(5):e97224. https://doi.org/10.1371/journal.pone.0097224.